

Characteristics of Cone-Forming Cyanobacteria and Implications for the Origin of Conical Stromatolites

by

Alexander Joseph Evans

B.S.E., University of Michigan (2006)

Submitted to the Department of Earth, Atmospheric and Planetary Sciences
in partial fulfillment of the requirements for the degree of

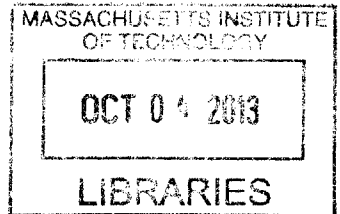
Master of Science

at the

MASSACHUSETTS INSTITUTE OF TECHNOLOGY

September 2013

ARCHIVES



© Massachusetts Institute of Technology 2013. All rights reserved.

Handwritten signature

Author
Department of Earth, Atmospheric and Planetary Sciences
August 26, 2013

Certified by
Tanja Bosak
Cecil and Ida Green Assistant Professor of Geobiology
Thesis Supervisor

Accepted by
Robert D. van der Hilst
Schlumberger Professor of Earth Sciences
Head, Department of Earth, Atmospheric and Planetary Sciences



Room 14-0551
77 Massachusetts Avenue
Cambridge, MA 02139
Ph: 617.253.2800
Email: docs@mit.edu
<http://libraries.mit.edu/docs>

DISCLAIMER OF QUALITY

Due to the condition of the original material, there are unavoidable flaws in this reproduction. We have made every effort possible to provide you with the best copy available. If you are dissatisfied with this product and find it unusable, please contact Document Services as soon as possible.

Thank you.

Some pages in the original document contain text that runs off the edge of the page.

Characteristics of Cone-Forming Cyanobacteria and Implications for the Origin of Conical Stromatolites

by

Alexander Joseph Evans

Submitted to the Department of Earth, Atmospheric and Planetary Sciences
on August 26, 2013, in partial fulfillment of the
requirements for the degree of
Master of Science

Abstract

Dating back to 3.5 Gya, stromatolites, which are composed of laminated and lithified carbonate rock, may contain the earliest records of phototaxis, photosynthesis, and oxygenation of the environment. The reconstruction of the co-evolution of biology and the environment using stromatolites depends on the ability to recognize macroscopic shapes that arise uniquely as a consequence of microbial processes. Our investigation aims to understand the biological factors in the formation of conical structures and stromatolites. To elucidate the role of the cyanobacteria, we enrich cyanobacteria from modern hot-spring communities of cone-forming microbes and subsequently test how the formation of conical structures depends on individual strains of the community. In our analysis, we augment morphological identification by genomic analyses of the 16S ribosomal DNA. Through a combination of mixing isolated heterotrophic bacteria and enriched filamentous cyanobacteria communities, we find that heterotrophic bacteria are a determinative factor in the formation and morphology of conical structures. Further, our experiments show the mere presence of a thin, filamentous cone-forming cyanobacteria phenotype is not a sufficient condition for cone formation.

Part of this work has been published as:

Sim, M. S., Liang, B., Petroff, A. P., Evans, A., Klepac-Ceraj, V., Flannery, D. T., et al. (2012). Oxygen-Dependent Morphogenesis of Modern Clumped Photosynthetic Mats and Implications for the Archean Stromatolite Record. Geosciences, 2(4), 235259. doi:10.3390/geosciences2040235;

Bosak, T., Liang, B., Wu, T. D., Templer, S. P., Evans, A., Vali, H., et al. (2012). Cyanobacterial diversity and activity in modern conical microbialites. Geobiology, 10(5), 384401. doi:10.1111/j.1472-4669.2012.00334.x.

Thesis Supervisor: Tanja Bosak

Title: Cecil and Ida Green Associate Professor of Geobiology

Acknowledgments

I would like to express my deepest appreciation to all those who provided me the possibility to complete this report. With special gratitude, I thank Tanja Bosak, whose contribution in stimulating suggestions and encouragement helped me to coordinate my project especially in writing this report. I would also like to thank undergraduates B. Dylan Bannon and Xinchu Yin who provided valuable contributions to this work. I thank fellow lab group members Biqing Liang, Min Sub Sim, Stefanie Templer for the support, assistance, and instruction. Last but not least, many thanks go to my thesis committee: Tanja Bosak, Brad Hager, Shuhei Ono, Taylor Perron, and Maria Zuber.

Contents

1	Introduction	15
2	Methodology	19
2.1	Growth	19
2.2	Cyanobacteria Enrichment Techniques	20
2.2.1	Antibiotic Selection	20
2.2.2	Flow Cytometry	20
2.2.3	Motility: Scoring of Agar Plate	21
2.3	Selection of Heterotrophic Bacteria	21
2.4	DNA Analysis & Clone Libraries	22
2.5	Chlorophyll Extraction & Analysis	23
2.6	Protein Extraction & Analysis	23
3	Results & Discussion	27
3.1	Enrichment Cultures	27
3.1.1	Selection	27
3.1.2	Clone Library from Single Culture	27
3.1.3	Enrichment Comparison	28
3.1.4	Motility	29
3.1.5	Chlorophyll & Protein Analysis	29
3.2	Community & Heterotrophic Bacteria Mixing	30
4	Summary	43

4.1	Conclusions	43
4.2	Future Work	44
5	Appendix A: Other Methods for Selection	45
5.1	Selection and Characterization of Cyanobacteria	45
5.2	Isolation of Heterotrophic Bacteria	46
6	Appendix B: Growth Conditions & Observations of Cyanobacterial Commu-	
	nity Enrichment Cultures	47
6.1	Standard Conditions	47
6.2	Low Light	48
6.3	Low Water Depth	49
6.4	Anaerobic	49
6.5	Microscopy	50

List of Figures

- 2-1 Selection of cyanobacteria. (a) First step in antibiotic selection. A photograph of a culture plate with an antibiotic disc placed on a top layer of agar with sample. Growth on the disc is observed by the Zeiss Axioplan Microscope. (b) Second step in antibiotic selection. The old antibiotic disc (with cyanobacteria) is placed closely next to a new antibiotic disc in the presence of a light gradient to stimulate growth towards the new disc. This step is repeated at least twice. (c) Agar plates scored with the dry calcium-alginate swabs. Dashed lines indicate the path of the scored lines where cyanobacterial growth was detected. Circles indicate location of enrichments that were grown in aerobic medium. The light gradient induces growth away from the initial inoculation site. 24
- 2-2 Epifluorescence images of scored agar plates. Samples from NB2 were inoculated to Plate NCC01 and NCC02 on top of the scored agar. The change in growth orientation and movement can be observed near the inoculation site (a) and (b). Further removed from the inoculation site, Plate NCC01 is observed to be following the scoring of the agar (c). Samples were enriched at the farthest front to promote enrichment as shown in (d), (e), (f). 25
- 3-1 DNA base pair principal component analysis. Our enrichment samples (1-25) are compared with the Yellowstone National Park samples of [Bosak et al., 2012], samples 26-36. The distance shown on the plot corresponds to evolutionary base pair differences. 32

3-2	Image of culture used for morphological analysis. Sample contains two types of conical structures: light green, fluffy tufted structures and dark green, dense conical structures.	33
3-3	Image from [Bosak et al., 2012]. Vertical aggregation in enrichment cultures of motile filamentous cyanobacteria from YNP. Vertical structures in the cultures of enrichment 1 (XAN-1) contain approximately 0.5 mm wide dense central aggregates draped by filmy biofilms on the side. Enrichment (XAN-12) filaments are brown, exhibit possible phycoerhythrin autofluorescence, and form lawns of filmy vertical structures. Enrichment (XAN-8) forms horizontal filmy mats that enclose numerous bubbles (arrows). FYG forms filmy structures and is present in various vertical structures (Bosak et al., 2009, 2010). Scale bar: 4 mm.	34
3-4	Epifluorescence images of scored agar plates (7 to 10-day incubation). (a). Enrichment 1 image of thick, dense cyanobacterial layer coverage. (b) Image of multiple chained cyanobacterial clumps in enrichment 8. (c) Image with thin, layered cyanobacterial filaments in enrichment 12 (d) Image with multiple layers, thinned areas, and scattered clumps of cyanobacteria in enrichment 14.	35
3-5	Filament motility (mm/hr). The plot shows the distance traveled by filamentous gliding cyanobacteria from enrichments 1, 8, 12, and 14 over 72 hours. The data were recorded by epifluorescence microscopy at 16-hr and 19-hr intervals on scored agar plates.	36
3-6	Chlorophyll <i>a</i> & protein ratios for high, medium and low light conditions after one week. Measurements were taken from filter triplicates and the error bars represent the standard error on the mean. Ratios were also calculated after 5 days at high light conditions - high (midway). (a). Chlorophyll <i>a</i> is plotted for enrichments 1, 8, 12, and 14 as a ratio of the final to initial amount of chl <i>a</i> present. (b). Protein is plotted for enrichments 1, 8, 12, and 14 as a ratio of the final to initial amount of protein present.	37

3-7	Mixing of cyanobacteria (28-day incubation). Different enrichments were mixed based on day 0 in a 1:1 protein ratio. (b) Mixed enrichments 1 and 8. (d) Mixed enrichments 1 and 14. (f) Mixed enrichments 8 and 14. Also shown are control standards: (a) Enrichment 1 (b) Enrichment 8 (c) Enrichment 14. Scale bar: 1 cm.	38
3-8	Mixing of heterotrophic bacteria with cyanobacteria (28-day incubation). Heterotrophic bacteria were added to cyanobacterial enrichments on day 0 in a 1:1, 1:10, and 1:100 protein ratio. More cones developed in cultures that contained lower heterotrophic bacteria to cyanobacteria initial protein ratios. These cultures also exhibited a greater spacing consistency and greater homogeneity. Scale bar: 1 cm.	39
6-1	Enrichment 1 (14-day incubation). Growth of enrichment 1 at nominal aerobic, low water anaerobic, low water aerobic, and low light aerobic conditions, respectively.	51
6-2	Enrichment 8 (14-day incubation). Growth of enrichment 8 is shown at nominal aerobic, low water anaerobic, low water aerobic, and low light aerobic conditions, respectively.	52
6-3	Enrichment 14 (14-day incubation). Growth of enrichment 14 is shown at nominal aerobic, low water anaerobic, low water aerobic, and low light aerobic conditions, respectively.	53

List of Tables

3.1	Isolated heterotrophic bacteria samples	40
3.2	Clone library.	41
6.1	Average filament length	54

Chapter 1

Introduction

Attached, laminated, and lithified carbonate rocks that dominated shallow marine environments for the majority of Earth's history preserve a record of the early Earth environment [Grotzinger and Knoll, 1999, Hofmann, 1973, Hofmann et al., 1999, Awramik, 1992]. While modern stromatolites accrete by sediment trapping and/or in-situ precipitation induced by microbial or algal activity [Altermann and Schopf, 1995, Awramik and Riding, 1988, Burne and Moore, 1987, Dupraz and Visscher, 2005, Gischler et al., 2008], the processes governing the highly variable macroscopic morphology of stromatolites are not fully understood [Grotzinger and Knoll, 1999, Bosak et al., 2013]. Traditionally, the upward migration of microbes in conical stromatolites had been attributed to phototaxis [Walter et al., 1976a, Awramik and Vanyo, 1986]; however, recent numerical modeling of modern conical microbialites indicate that conical morphology may instead be the result of nutrient limitation [Petroff et al., 2010].

Modern-day conical stromatolites are rare and are constrained generally to sites with high temperatures and low current energy such as the hot springs of Yellowstone National Park (YNP) [Jones et al., 2002, Lau et al., 2005, Bosak et al., 2012]. [Walter et al., 1976b, Bosak et al., 2009, Bosak et al., 2010, Lau et al., 2005] identify thin filamentous cyanobacteria as a key constituent in modern conical microbialites. Modern conical microbialites observed in the YNP hot springs appear morphologically similar to Archean and Proterozoic

conical stromatolites and exhibit similar characteristics: slopes greater than 30°, crestral thickening, and a consistent pattern of lattice spacing [Wharton et al., 2013, Petroff et al., 2010, Petroff et al., 2013, Bosak et al., 2013].

From genomic analysis of cyanobacterial diversity, Lau et al. (2005) suggested conical microbialites may require the presence of unicellular cyanobacteria unique to cone structures, yet absent from the surrounding mat. Though these observations suggested that the microbial populations in conical structures did not vary vertically or distinctly between different cone morphologies, the more comprehensive analysis of Bosak et al. (2012) found more diverse filamentous cyanobacteria in the cones relative to the surrounding mat and some filaments that seemed to occur only in cones. Furthermore, while Bosak et al. (2012) observed a relative enhancement in filamentous cyanobacteria present in cone structures, they did not find any cone-specific unicellular cyanobacteria in contrast to Lau et al. (2005). Hence, the presence of unicellular cyanobacteria cannot be a sufficient condition for the formation of cone morphologies and instead may be determined by other factors (e.g., [Reyes et al., 2013]).

Past studies have focused on cyanobacterial diversity and activity [Hofmann, 1973, Awramik and Vanyo, 1991, Lau et al., 2005, Walter et al., 1976b, Bosak et al., 2012, Reyes et al., 2013], processes such as nutrient limitation [Petroff et al., 2010, Petroff et al., 2013] and oxygen cycling [Sim et al., 2012]. These studies explained lattice spacing and clumping behavior in modern-day conical microbialites and other stromatolites. The identification of nutrient limitation and oxidative stress indicates that the environment and biotic community jointly influence stromatolite morphology. Herein, we investigate the relationship between the general microbial community and distinct cone morphologies. Thus, the non-cyanobacterial community may also be a contributing factor in the formation and development of conical stromatolites.

To elucidate the role of filamentous cyanobacteria, we test whether the formation of conical structures is a consequence of an individual cyanobacterial strain, growth conditions, or a community. Our analysis focuses on the microbial interactions between the cyanobacterial and heterotrophic components within the cone-forming community under a variety of environmental conditions. We view this as a necessary, yet preliminary analysis in the

deconvolution of environmental and biotic factors influencing conical stromatolite development.

Chapter 2

Methodology

The samples used in this study were collected from Yellowstone National Park in September 2008 under permit #YELL-2008-SCI-5758 as described in [Bosak et al., 2009].

2.1 Growth

Motile, filamentous cyanobacteria were enriched by serial harvesting, selection of the fastest-gliding filaments, and culturing of cones in the modified Castenholz medium D containing lower concentrations of nitrate and phosphate (2.3 mM NO_3^- and 0.8 mM PO_4^{3-} , respectively) at pH 8 [Castenholz, 1970, Bosak et al., 2012]. These organisms were identified as cyanobacteria using 16S rDNA sequences and Chl*a* autofluorescence. The medium was equilibrated with an anaerobic atmosphere (90% N_2 , 5% CO_2 and 5% H_2) or atmospheric air, respectively. The anaerobic medium received an additional 2.2 g NaHCO_3 per liter, and all media were titrated with NaOH or HCl to an initial pH of 8. Enrichment cultures were grown at 45°C in an aerobic incubator or in an anaerobic glove box (Coy Manufacturing Co., Ann Arbor, Mich.) on solid surfaces consisting of silica sand, aragonite sand or agar with capped plastic or glass culture containers. The glass culture containers were sealed using paraffin film to prevent evaporation and allow gas exchange. Containers were placed at different distances from the cool white fluorescent light source (26 W with a 12h light:

12 h dark cycle) at 10, 50 and 160 E/m²/s to characterize growth at low, medium, and high light intensities, respectively.

2.2 Cyanobacteria Enrichment Techniques

We investigated three methods of cyanobacteria isolation from phototactic enrichments: antibiotic selection, flow cytometry, and motility.

2.2.1 Antibiotic Selection

We plated samples of the enrichment on modified Castenholz-D medium (solidified by 2% agar) containing a variety of antibiotic discs (manufactured by Becton, Dickinson and Company, Sparks, Maryland): Ampicillin-10, Bacitracin-10, Chloramphenicol-30, Colistin-10, Erythromycin-15, Kanamycin-30, Novobiocin-30, Streptomycin-10, Tetracycline-30, and Vancomycin-30. Cells dispersed in 15mL of 0.5% agar solution were applied to the culture plate containing three different antibiotic discs on a 1% agar surface. Susceptibility to each antibiotic was identified by measuring the radius of the reduced growth zone surrounding the antibiotic disc. Antibiotic discs that demonstrated a zone of susceptibility were analyzed for growth within the zone. Any growth in the zone was re-inoculated to a new culture plate with a fresh antibiotic disc to further test resistance (Figure 2-1). The sample and antibiotic disc were placed in a low light gradient to further promote phototactic enrichment of the final enrichment. This method was repeated twice and final enrichments were grown in liquid culture medium without antibiotic.

2.2.2 Flow Cytometry

Because cone-forming cyanobacteria grow as filaments and form clumps and/or cohesive structures, we filtered the samples before separation to attain single, isolated cells. Fluorescent dye was applied to cells to distinguish between live and dead populations using the

LIVE/DEAD BacLight Bacterial Viability and Counting Kit (Invitrogen, Carlsbad, CA). Flow cytometry was conducted at the Dana-Farber Cancer Institute Flow Cytometry Core Facility at Harvard University. The cells were plated on culture plates (2% agar). Growth was monitored microscopically using cyanobacterial auto-fluorescence and a Zeiss Axioplan Microscope. The newly grown cells were inoculated on new culture plates using Luria-Bertani (LB) broth and aerobic Castenholz-D agar solutions.

2.2.3 Motility: Scoring of Agar Plate

We scored the surface of a modified Castenholz-D agar (2%) plate with parallel lines using a dry calcium alginate swab [Burton and Lee, 1978, Vaara et al., 1979]. We aligned the parallel lines with a light gradient to further promote the enrichment of the phototactic, filamentous, gliding cyanobacteria. A small sample was placed on the scored path near the dark end of the plate. Plates were incubated for at least one day. Filaments that glided along the scored path, shown in Figure 2-1c, were identified by the use of a Zeiss Axioplan Microscope and cultured in liquid Castenholz-D medium. After incubation, three plates each scored nine times, contained cyanobacteria that had glided away from the original inoculation site (Figure 2-1c). These samples were immediately extracted from the culture plate with the use of a sterile scalpel and inoculated to modified Castenholz-D medium at 45° C. Epifluorescence microscopy indicated that these were samples that contained a single filament cyanobacteria (Fig 2-2).

2.3 Selection of Heterotrophic Bacteria

Enrichment cultures grown in the absence of light were inoculated on a 1% agar plate of 2.5-g/L Luria-Bertani (LB) broth, 1.08-g/L Xylan from beechwood, .9-g/L fructose and glucose, or 0.4-g/L glycolic acid. A sterile cotton swab was used to inoculate the enrichment to the center of the plate and the area was marked on the agar plate and wrapped with parafilm and aluminum foil. Plates were placed in 45° C aerobic incubator for at least three

days. A sterile toothpick was used to collect isolated colonies from the agar plate and used to transfer the colony into a culture vial with 3 mL of liquid medium. Vials were placed on an orbital shaker (VWR, Radnor, PA) at 400 rpm in 45° incubator. Once growth was visible, samples were re-inoculated on 1% agar plate and the selection process repeated at least once.

2.4 DNA Analysis & Clone Libraries

We conducted DNA analysis for identification using 16S rDNA [Ward et al., 1997, Gallagher et al., 2004, Goh et al., 2008, Foster et al., 2009]. Clone libraries are used to estimate the relative genetic diversity of a community and may be associated with a particular phenotype or growth condition. All centrifugation steps for this procedure were conducted at 14,800 rpm. Approximately 0.25-1 g of biofilm was excised from each culture and aggregates were dispersed with a sterile scalpel blade. Genomic DNA was extracted using the Mo-bio UltraClean Soil DNA Isolation Kit (Mo Bio Laboratories, Inc, Carlsbad, CA). The DNA was tested for purity and concentration in a NanoDrop (Thermo Scientific, Wilmington, DE). We used the PCR (polymerase chain reaction) to amplify DNA from the prior step using universal primers 27F (5'-AGAGTTTGATYMTGGCTCAG-3')/1492R (5'-TACGGYTACCTTGTTACGACTT-3') [Hoefel et al., 2005]. The Invitrogen TOPO TA Cloning Kit was used according to the manufacturers instructions. The PCR amplifications were performed with the MyCycler thermocycler (Bio-Rad Laboratories, Hercules, CA). The cycle parameters included an initial denaturation at 95°C for 4 min; 30 cycles of denaturation at 95°C for 35 s, annealing at 45°C for 55 s, and elongation at 72°C for 55 s; and a final 3-min elongation interval at 72°C. These 30 cycles denature the double-stranded DNA, anneal the primer to the single-stranded DNA, and the replicate the DNA, respectively. The amplified DNA was washed using the QIAprep Mini-Prep PCR Purification Kit (QIAGEN, Valencia, CA) and ligated into pCR4-TOPO vector (Invitrogen, Carlsbad, CA), according to the instructions and introduced into *E. coli* by electroporation. Plasmids were extracted from ampicillin-resistant colonies using the QIAprep Mini-prep Plasmid Purification Kit.

The target DNA was sequenced at the MIT CCR Biopolymers Laboratory using primers T3 (5'-ATTAACCCTCACTAAAGGGA-3') / T7 (5'-TAATACGACTCACTATAGGG-3'). The Basic Local Alignment Search Tool (BLAST) of the National Center for Biotechnology Information (National Institutes of Health) was used to align our sequences. Sequences were compared to nearest identified relatives and one another.

2.5 Chlorophyll Extraction & Analysis

Samples were inoculated in triplicate with 0.2 mL of enrichment culture and placed on a 5-micron filter and divided into halves and used for protein and chlorophyll analysis. Per [Hagerthey et al., 2006], samples were freeze-dried for at least 48 hours and steeped in 1 mL of methanol/acetone/DMF/water (30:30:30:10) for 2 hours at 4°C. Subsequently, samples were sonicated 5-10 times with 5 second pulses and centrifuged for 5 minutes at 9900 rpm and at 4°C. A 750 µL of supernatant was spectrally analyzed. The total amount of chl *a* was calculated at the beginning and end of each experiment by

$$CHL_a = 11.64A_{665} - 2.16A_{645} + 0.10A_{630}. \quad (2.1)$$

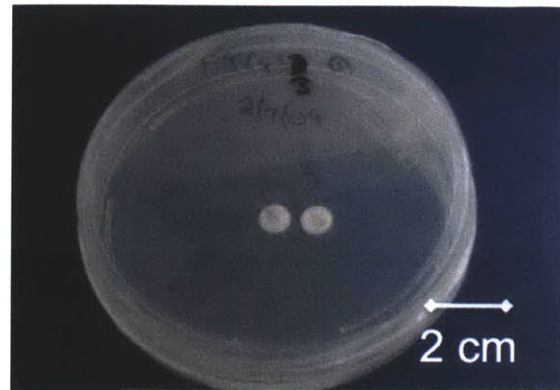
We use the ratio of chlorophyll at the end and start of the experiment to quantify the difference in chlorophyll.

2.6 Protein Extraction & Analysis

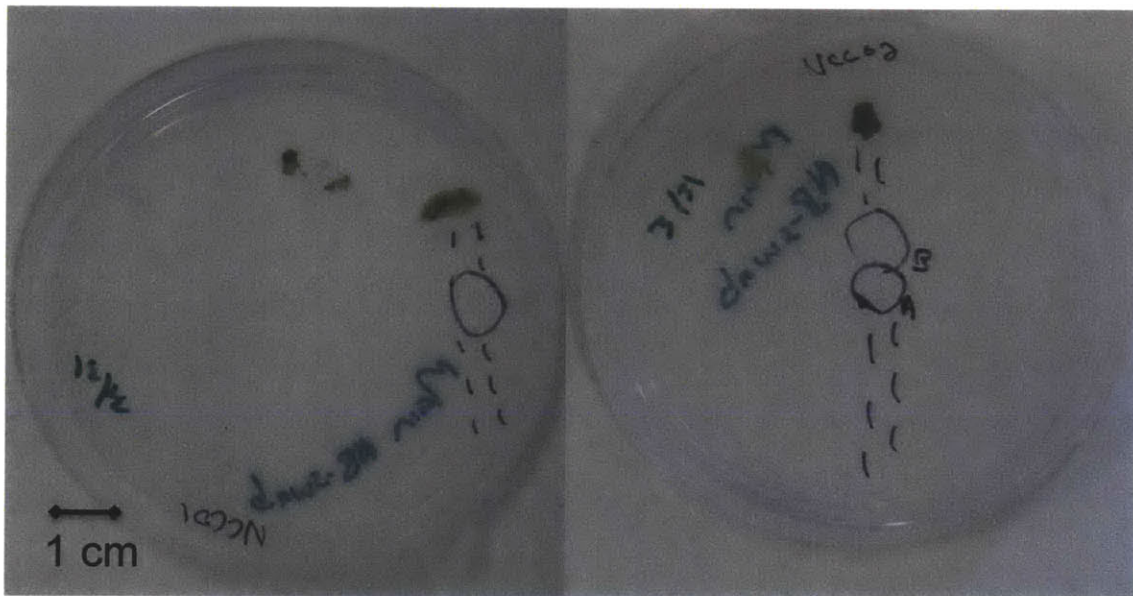
Samples were inoculated in triplicate with 0.2 mL of enrichment mixture and placed on a 5-micron filter and divided into two even pieces used for protein and chlorophyll analysis. The filter samples were immersed in 1N NaOH and heated to 90°C for 10 minutes. The supernatant was used for protein quantification in the Quant-iT Protein Assay Kit (Life Technologies, Grand Island, NY) and calculated by a linear extrapolation from provided standards.



(a) First step in antibiotic selection.

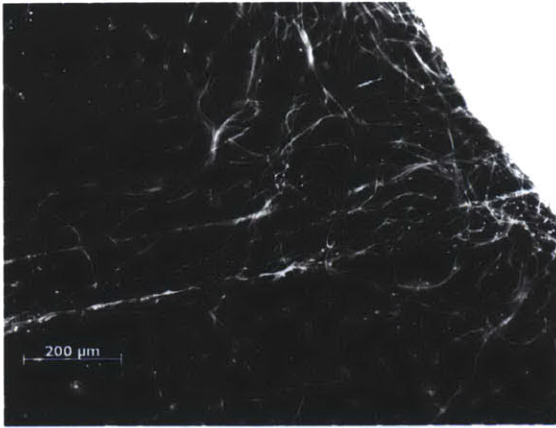


(b) Second step in antibiotic selection.

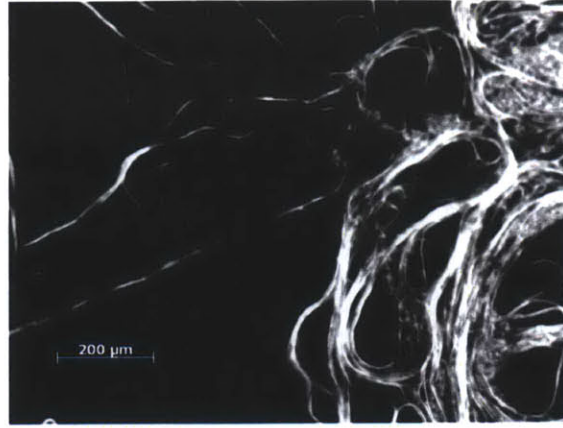


(c) Scoring of agar plate

Figure 2-1: Selection of cyanobacteria. (a) First step in antibiotic selection. A photograph of a culture plate with an antibiotic disc placed on a top layer of agar with sample. Growth on the disc is observed by the Zeiss Axioplan Microscope. (b) Second step in antibiotic selection. The old antibiotic disc (with cyanobacteria) is placed closely next to a new antibiotic disc in the presence of a light gradient to stimulate growth towards the new disc. This step is repeated at least twice. (c) Agar plates scored with the dry calcium-alginate swabs. Dashed lines indicate the path of the scored lines where cyanobacterial growth was detected. Circles indicate location of enrichments that were grown in aerobic medium. The light gradient induces growth away from the initial inoculation site.



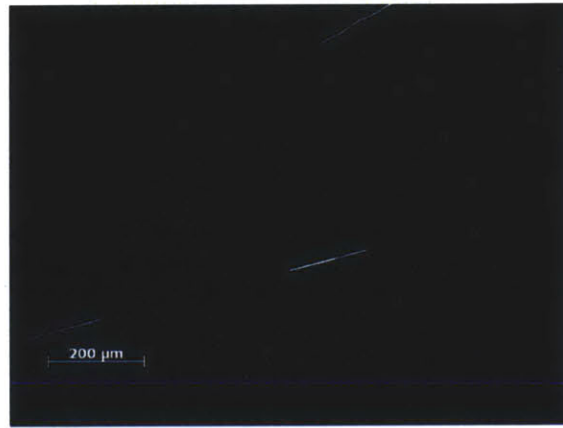
(a) Plate NCC01 - Inoculation Site.



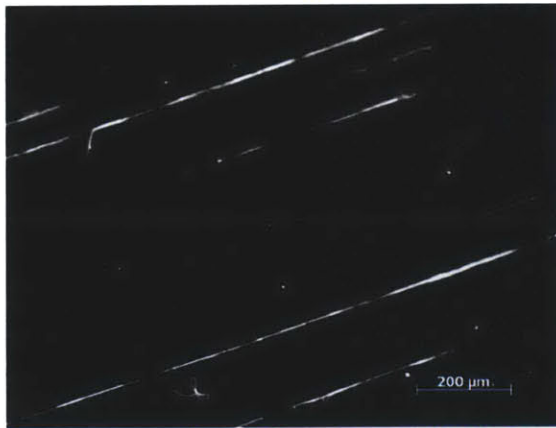
(b) Plate NCC02 - Inoculation Site.



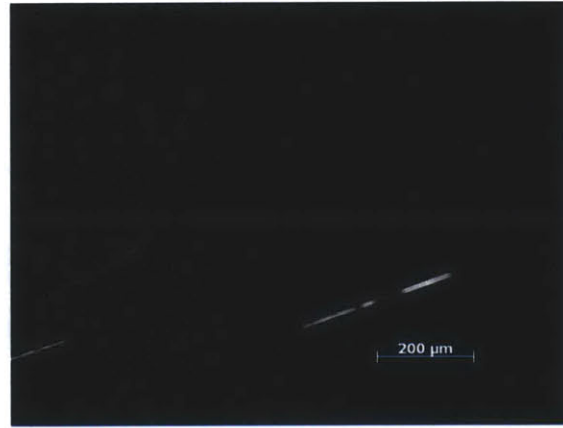
(c) Plate NCC01 - Between inoculation and sample collection sites



(d) Plate NCC02 - Sample Collection Site A



(e) Plate NCC01 - Sample Collection Site.



(f) Plate NCC02 - Sample Collection Site B.

Figure 2-2: Epifluorescence images of scored agar plates. Samples from NB2 were inoculated to Plate NCC01 and NCC02 on top of the scored agar. The change in growth orientation and movement can be observed near the inoculation site (a) and (b). Further removed from the inoculation site, Plate NCC01 is observed to be following the scoring of the agar (c). Samples were enriched at the farthest front to promote enrichment as shown in (d), (e), (f).

Chapter 3

Results & Discussion

3.1 Enrichment Cultures

3.1.1 Selection

Taking advantage of the thin filamentous cyanobacterial gliding motility and phototaxis, we inoculated samples to a scored agar plate to promote unidirectional movement. Using this method, we isolated over 20 non-unique cyanobacterial enrichments. We use principle component analysis (PCA) of the base-pair sequences for cyanobacteria in each community along with cyanobacteria identified in Yellowstone in 2010 [Bosak et al., 2012] to identify sequence differences (Figure 3-1). For our analyses, we use cyanobacterial enrichments 1, 8, 12, and 14.

We isolated three unique heterotrophic bacteria (Table 3.1).

3.1.2 Clone Library from Single Culture

^a In aerobically incubated samples, we observed morphologically different conical structures within the same culture (Figure 3-2). As the origin of this difference is unlikely to

^aPart of this subsection was published in [Sim et al., 2012].

be environmentally induced, we analyzed and compared enrichments of the two different morphological structures: fluffy, tufted aggregates and small dark-green, compact cones. We compared the tuft structures (CL2), the compact cone structures (CD), and a mixture of the aforementioned structures (CM). Additionally, we analyzed morphologically similar structures to the dense dark green cones from a separate culture (DC2).

We obtained too few clones to make statistically significant conclusions from the results of the clone library (shown in Table 3.2). However, these data suggest that morphologically distinct populations can contain the same dominant cyanobacterial phylotype with the same cyanobacteria, *Leptolyngbya*, present in the dense dark cones and tufted aggregates.

Bacterial 16S rRNA gene sequences in compact cones, tufts and mixed morphologies suggest the presence of expanded niches for non-photosynthetic organisms in compact cones. Clone libraries from tufts, compact cones and mixed morphologies contained similar 16S rRNA gene sequences of thin filamentous non-heterocystous cyanobacteria from Subsection III of [Bosak et al., 2012]. Cyanobacterial clones comprised 87% of all clones in tufts, but only 16% in the compact cone structures (Figure 3-2).

The relative percentage of cyanobacteria decreased with increased concentration of the compact cones. Most sequences in the compact cones were instead similar to non-photosynthetic heterotrophic organisms and were more diverse than the sequences of non-photosynthetic organisms in tufts. The relative percentage of the heterotrophic bacteria increased in compact cones and may be a significant factor in the observed morphological difference. We examine this concept further in Section 3.2.

3.1.3 Enrichment Comparison

Enrichments 1,8, 12 and 14 contain different filamentous cyanobacteria and are capable of producing conical structures with differing morphologies. Unlike the other enrichments, enrichment 8 only developed cones at very shallow water depths and readily clumped at the macro- and micro- scales (see Figure 3-4 and Appendix B). The lack of cones in enrichment 8 may be related to the ability of enrichment 8 to easily disperse itself in clumps throughout

the water column with respect to enrichment 1 and 14 (see Appendix B). This is consistent with the aerobic growth conditions (Appendix B) in which enrichment 14 does not form cones, but instead readily disperses growth within the water column. Given the expected nutrient limitation as a precursor to cone formation as suggested by [Petroff et al., 2010], the propensity of enrichment 8 to disperse clumps throughout the water column may better enable the enrichment to overcome diffusive limitations, for example with inorganic carbon uptake, at the solid substrate surface and may be advantageous to cone development. This would be consistent with the cone development in enrichment 8 at low water levels, where clump dispersal throughout the water column is limited.

3.1.4 Motility

Cyanobacterial enrichments 1, 8, 12 and 14 were tested for differences in motility. Using the agar scoring method, we found that the average filament velocity for enrichment 8 was lower than enrichments 1, 12, and 14 at a 16-hr interval, although we found no statistical difference in velocity at a 19-hr interval (see Figure 3-5). The measurement differences at different intervals may arise from light-influenced motility differences instigated by the light cycle (12-hour light, 12-hour dark). The measurement difference may indicate increased phototactic sensitivity of enrichment 8 filament movement.

3.1.5 Chlorophyll & Protein Analysis

Because filamentous cyanobacteria clump, one cannot quantify the growth by standard cell counts or absorbance measurements. Therefore, we used chlorophyll and protein measurements to quantify cyanobacteria growth in enrichments 1, 8, and 14. Enrichment 8 produced more chlorophyll *a* per unit protein than other cyanobacteria. This may be an expected result if the development of cones is partly due to a phototactic response and enrichment 8 could offset the need of developing cones with an increased amount of chlorophyll per cyanobacterium.

Protein analysis showed there is 25-40 factor growth during the experiments under medium and high light conditions. There is a 8 to 12-factor increase in protein for filter experiments conducted at low light.

3.2 Community & Heterotrophic Bacteria Mixing

The addition of enrichment 8 to enrichment 1 or 14, respectively, reduced the number of cones per unit area (see Figure 3-7). In order to prevent contamination, we refrained from quantifying cone density in order to reduce exposure of the sample to the surrounding environment. The morphological differences between individual enrichments in Figure 3-7 and enrichment mixtures 1 & 8 and 8 & 14 suggest that the paucity of cones in the mixtures was not singularly due to enrichment 8 exhibiting its standard phenotype, but rather to interactions among communities. This can be observed in Figure 3-7, where the enrichment mixtures are morphologically different from the individual enrichment communities. Thus, given enrichments 1 & 14 produce cones, the paucity of conical structures in their mixtures with enrichment 8 cannot be due to the absence of a required type of filamentous cyanobacterium. This may also indicate the general absence of cones in enrichment 8 is due to the non-cyanobacterial community and enrichment 8 may contain a cone-forming inhibitor preventing the expression of conical structures.

We added isolated heterotrophic bacteria in 1:1, 10:1, and 100:1 protein ratio with respect to enrichments 1, 8, and 14. We focused on enrichment 1 with *Geobacillus* and enrichment 14 with *Flavobacteriales*. As indicated in Figure 3-8, a greater amount of *Geobacillus* inoculate in enrichment 1 resulted in cyanobacterial community growth without conical structures. A reduction in the amount of initial *Geobacillus* inoculate led to more homogeneous surface growth and an increase in the number of conical structures. Additionally, the same trend was observed with enrichment 14 and *Flavobacteriales*.

Our result is consistent with observations described in Section 3.1.2; the abundance of heterotrophic bacteria was found to alter cone formation. The reduction of conical structures was correlated with increased heterotrophic bacterial inoculate (i.e. *Geobacillus* and

Flavobacteriales). This is likely a result of the production of inorganic carbon and oxygen uptake of the heterotrophic bacteria [Petroff et al., 2010] which may prevent nutrient limitation for the cyanobacteria. If cone formation is partly a positive response to inorganic carbon limitation as suggested by [Petroff et al., 2010], this may explain the paucity of cones with higher inoculation concentrations of *Geobacillus* and *Flavobacteriales*.

Additionally, an increase in inoculate concentrations of *Geobacillus* and *Flavobacteriales* may enhance the removal of cyanobacteria-secreted extracellular polymeric substances (EPS) and cyanobacterial sheaths, thereby preventing cone formation. However, further work must be conducted on the distribution of EPS in enrichment mixtures with increased heterotrophic bacteria.

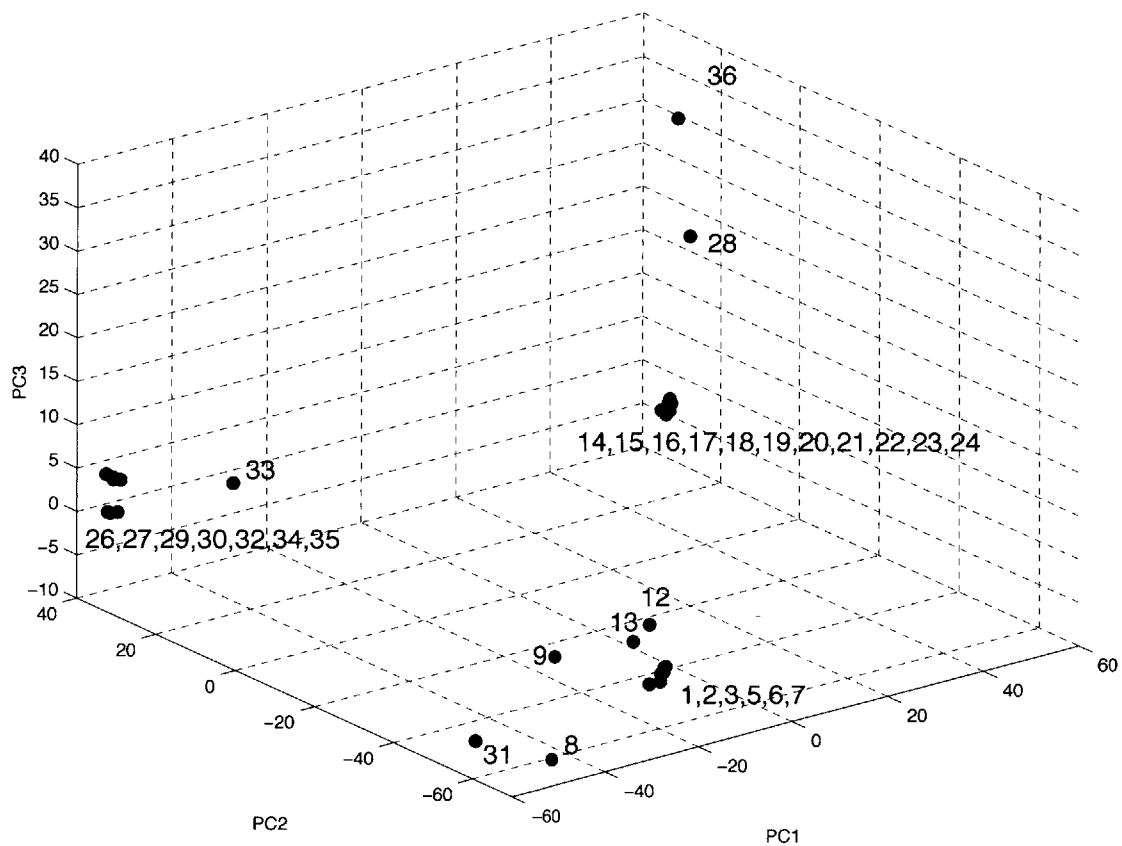


Figure 3-1: DNA base pair principal component analysis. Our enrichment samples (1-25) are compared with the Yellowstone National Park samples of [Bosak et al., 2012], samples 26-36. The distance shown on the plot corresponds to evolutionary base pair differences.

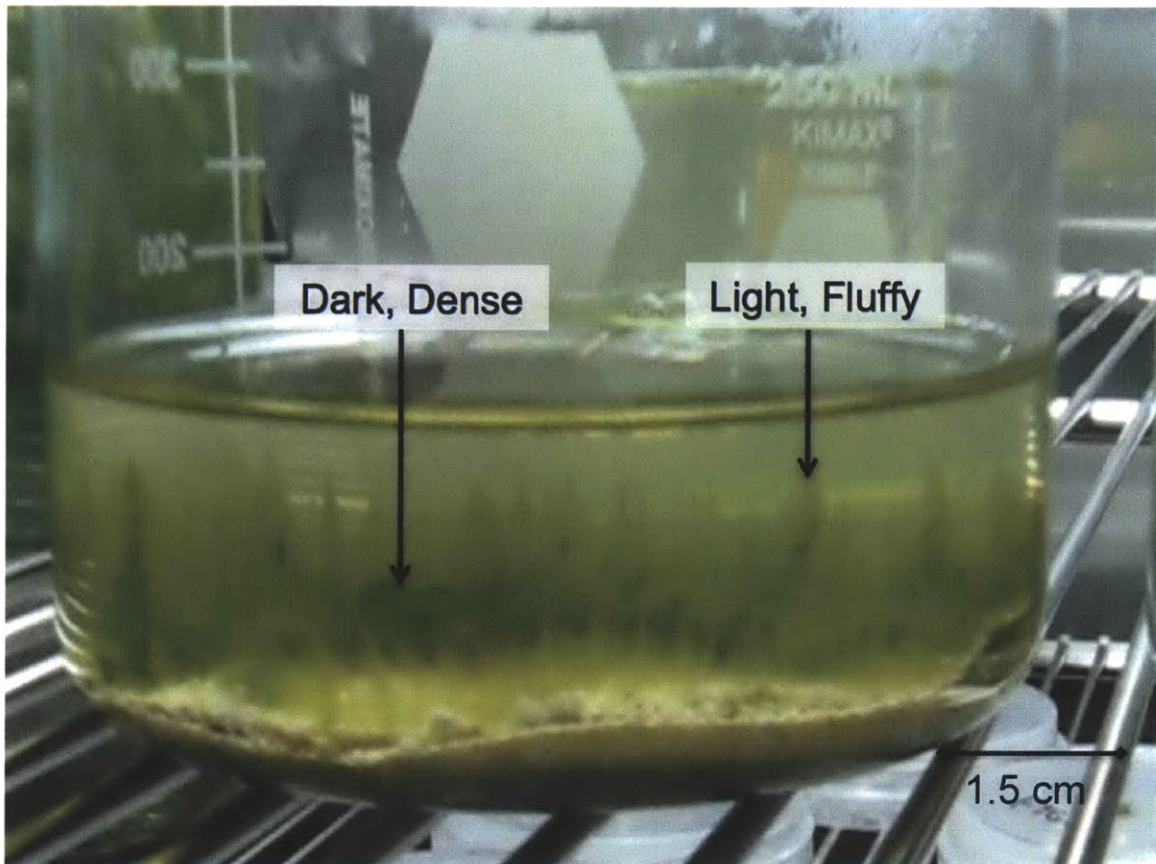


Figure 3-2: Image of culture used for morphological analysis. Sample contains two types of conical structures: light green, fluffy tufted structures and dark green, dense conical structures.

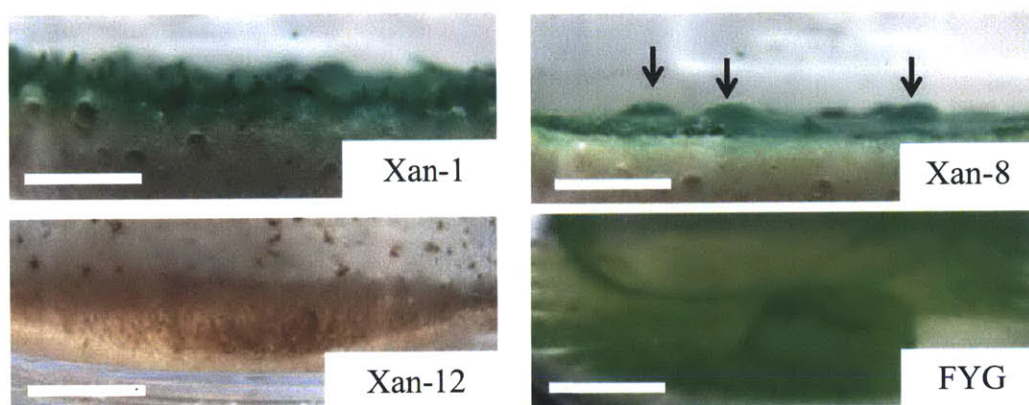
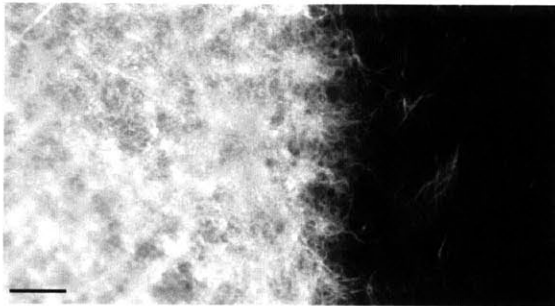
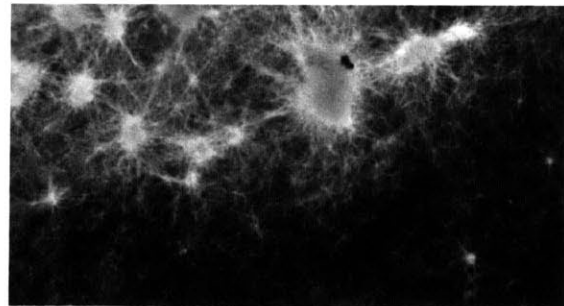


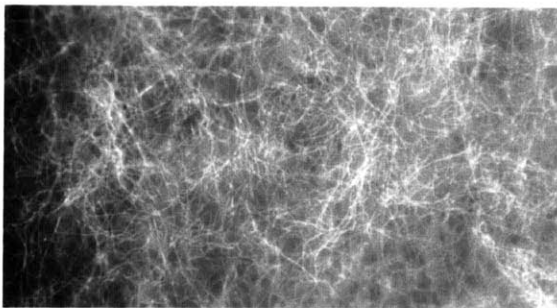
Figure 3-3: Image from [Bosak et al., 2012]. Vertical aggregation in enrichment cultures of motile filamentous cyanobacteria from YNP. Vertical structures in the cultures of enrichment 1 (XAN-1) contain approximately 0.5 mm wide dense central aggregates draped by filmy biofilms on the side. Enrichment (XAN-12) filaments are brown, exhibit possible phycoerhythrin autofluorescence, and form lawns of filmy vertical structures. Enrichment (XAN-8) forms horizontal filmy mats that enclose numerous bubbles (arrows). FYG forms filmy structures and is present in various vertical structures (Bosak et al., 2009, 2010). Scale bar: 4 mm.



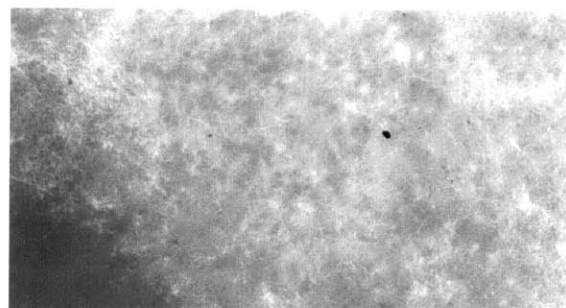
(a) Enrichment 1



(b) Enrichment 8



(c) Enrichment 12



(d) Enrichment 14

Figure 3-4: Epifluorescence images of scored agar plates (7 to 10-day incubation). (a). Enrichment 1 image of thick, dense cyanobacterial layer coverage. (b) Image of multiple chained cyanobacterial clumps in enrichment 8. (c) Image with thin, layered cyanobacterial filaments in enrichment 12 (d) Image with multiple layers, thinned areas, and scattered clumps of cyanobacteria in enrichment 14.

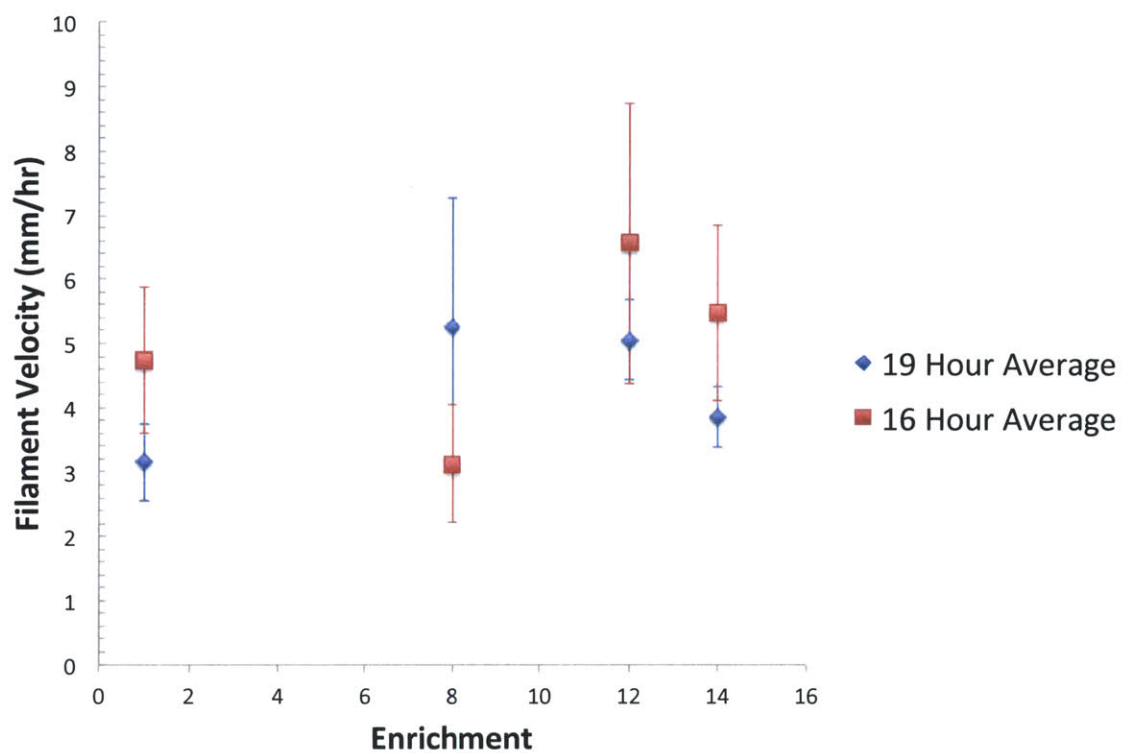
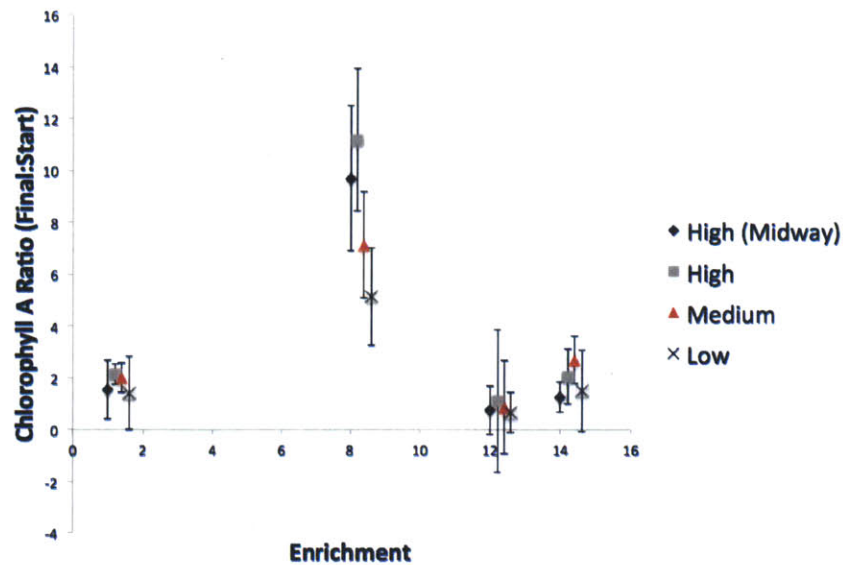
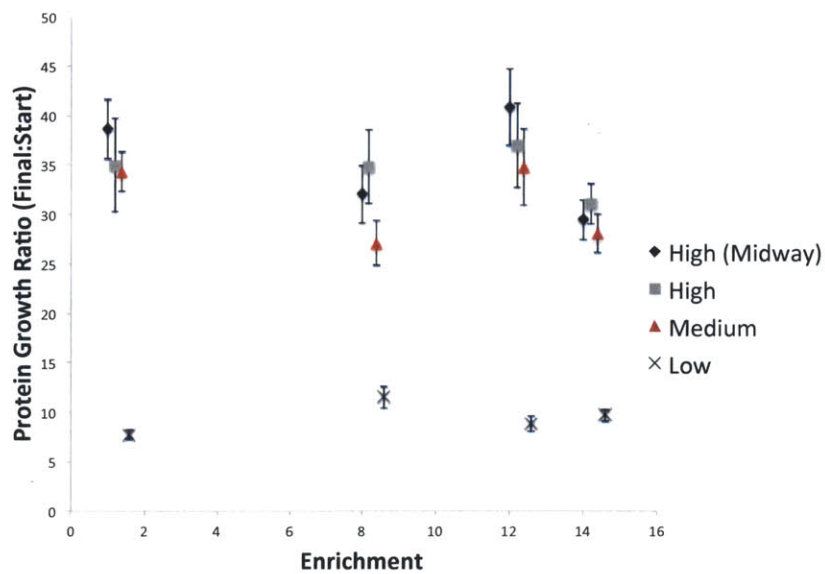


Figure 3-5: Filament motility (mm/hr). The plot shows the distance traveled by filamentous gliding cyanobacteria from enrichments 1, 8, 12, and 14 over 72 hours. The data were recorded by epifluorescence microscopy at 16-hr and 19-hr intervals on scored agar plates.



(a) Chla Growth Ratio



(b) Protein Growth Ratio

Figure 3-6: Chlorophyll *a* & protein ratios for high, medium and low light conditions after one week. Measurements were taken from filter triplicates and the error bars represent the standard error on the mean. Ratios were also calculated after 5 days at high light conditions - high (midway). (a). Chlorophyll *a* is plotted for enrichments 1, 8, 12, and 14 as a ratio of the final to initial amount of chla present. (b). Protein is plotted for enrichments 1, 8, 12, and 14 as a ratio of the final to initial amount of protein present.

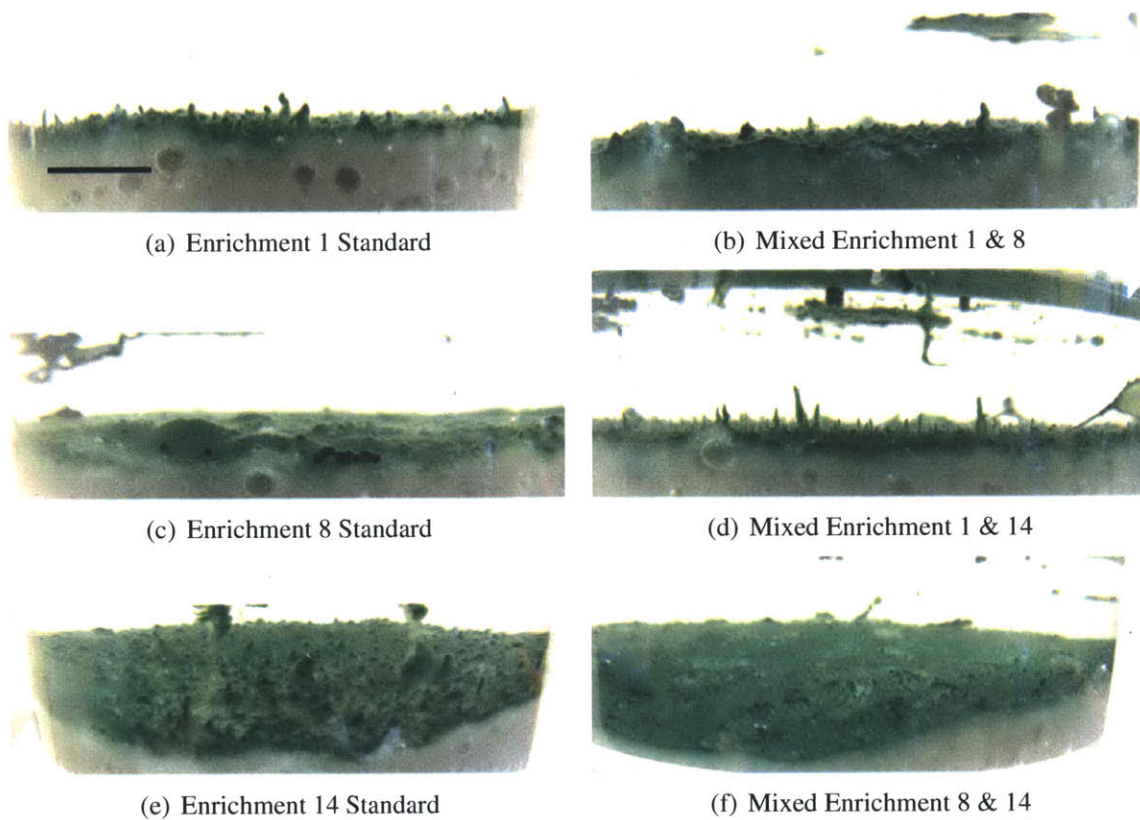


Figure 3-7: Mixing of cyanobacteria (28-day incubation). Different enrichments were mixed based on day 0 in a 1:1 protein ratio. (b) Mixed enrichments 1 and 8. (d) Mixed enrichments 1 and 14. (f) Mixed enrichments 8 and 14. Also shown are control standards: (a) Enrichment 1 (b) Enrichment 8 (c) Enrichment 14. Scale bar: 1 cm.

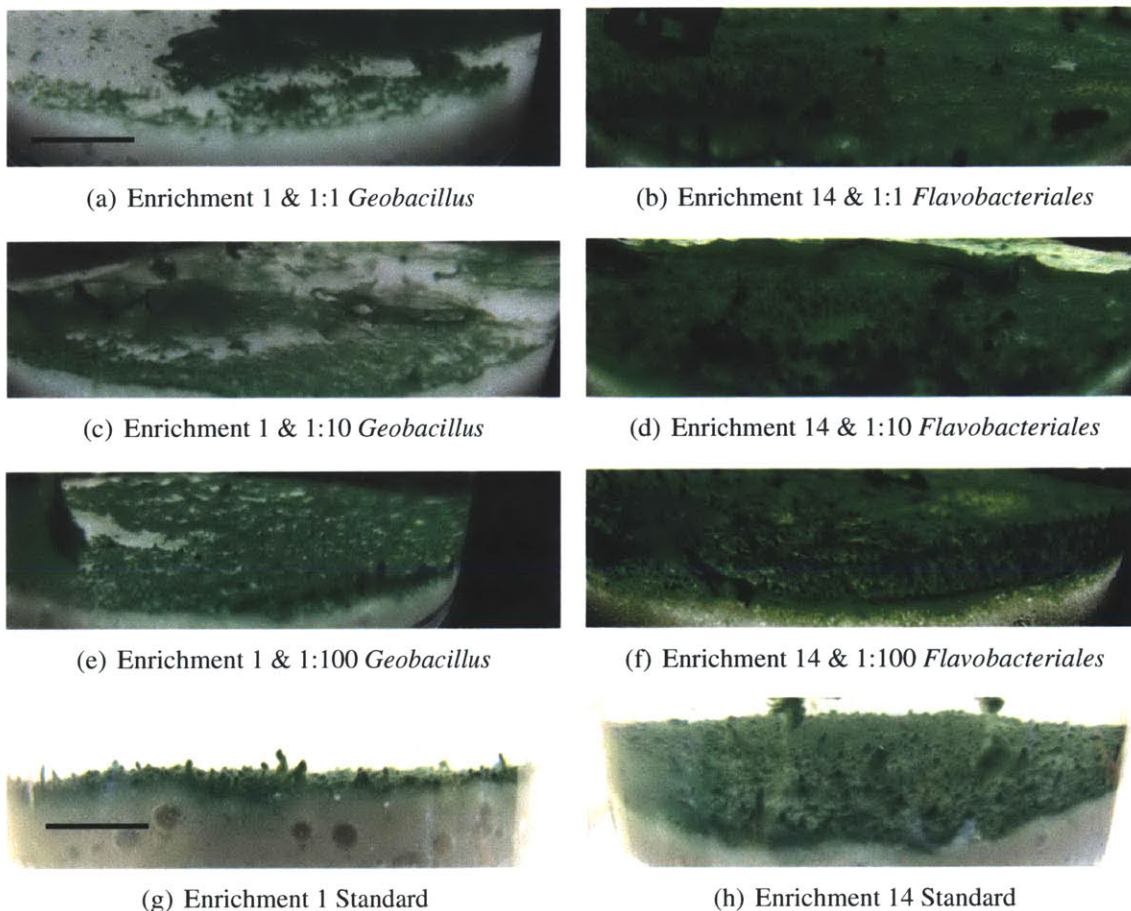


Figure 3-8: Mixing of heterotrophic bacteria with cyanobacteria (28-day incubation). Heterotrophic bacteria were added to cyanobacterial enrichments on day 0 in a 1:1, 1:10, and 1:100 protein ratio. More cones developed in cultures that contained lower heterotrophic bacteria to cyanobacteria initial protein ratios. These cultures also exhibited a greater spacing consistency and greater homogeneity. Scale bar: 1 cm.

Table 3.1: Isolated heterotrophic bacteria samples

Sample ID	Origin	Sequence		
		Nearest Relative(s)	Identity Match	Accession No.
A	14-27-LB	<i>Geobacillus</i>	99%	AY044053.1
B	1-ORANGE-LB	<i>Flavobacteriales</i>	99%	HQ172900.1
C	8-WHITE-LB	<i>Brevibacillus</i>	99%	KC493176.1
F	1-27-LB	<i>Flavobacteriales</i>	99%	HQ172900.1
K	02B1-27-LB	<i>Flavobacteriales</i>	99%	HQ172900.1

Table 3.2: Clone library.

Sample	Enrichment ID	Clones	Sequence		
			Nearest Relative(s)	Identity Match	Accession No.
Antibiotic Se- lection	NB2_1	10	<i>Cyanobacterium</i>	98%	EF429514.2
	NB2_1	10	<i>Leptolyngbya</i>	93%	AY493607.1
	NB2_15	1	<i>Geobacillus</i>	95%	EF466141.1
	NB2_16	1	<i>Burkholderia</i>	96%	DQ295805
Light	CL2_1	23	<i>Cyanobacterium</i>	98%	EF429514.2
	CL2_1	23	<i>Leptolyngbya</i>	93%	AY493607.1 DQ786166
Mixed	CL2_6	2	<i>Flaviobacteriales</i>	99%	HQ172900.1
	CM_1	12	<i>Cyanobacterium</i>	98%	EF429514.2
	CM_1	12	<i>Leptolyngbya</i>	93%	AY493607.1
	CM_8	2	<i>Flaviobacteriales</i>	99%	HQ172900.1
Dark	CM_8	6	<i>Burkholderia</i>	96%	EF648078.1
	CD_7	4	<i>Flaviobacteriales</i>	99%	EF648023.1
	CD_15	2	<i>Burkholderia</i>	99%	CP000152.1
	CD_17	3	<i>Gemmata</i>	93%	AM902596.1
	CD_18	2	<i>Cyanobacterium</i>	98%	EF429514.2
Dark Control	CD_18	2	<i>Leptolyngbya</i>	93%	AY493607.1
	DC2_25	3	<i>Flaviobacteriales</i>	99%	HQ172900.1
	DC2_24	1	<i>Iron-Reducing Bacterium</i>	94%	FJ269102.1

Chapter 4

Summary

4.1 Conclusions

By analyzing different combinations of isolated heterotrophic bacteria and enriched filamentous cyanobacteria communities, we find that heterotrophic bacteria play a role in the formation and morphology of conical structures. Further, we show that the mere presence of a thin, filamentous cone-forming cyanobacteria phenotype is not a sufficient condition for cone formation. Based on our results, we can make the following statements regarding conical microbialites:

1. The formation of conical structures does not require multiple thin, filamentous cyanobacteria.
2. The presence of unicellular and/or non-filamentous cyanobacteria is not a requirement for the formation of conical structures.
3. The morphology of conical microbialites may be strongly influenced and suppressed in the presence of abundant heterotrophic microbes.

Reconstruction of the paleoenvironment based on conical stromatolites necessitates an understanding of the diversity of the stromatolite bacterial community. While phototaxis and clumping by cone-forming cyanobacteria are undoubtedly factors in the development of

conical structures, the final morphology of the conical structures are strongly correlated with the presence of non-cyanobacterial organisms in the community.

Our results support the notion that upward motility, commonly attributed to only phototaxis, is likely a response to a nutrient or other chemical species in a diffusion-limited gradient [Petroff et al., 2010]. The upward gliding of filaments along other untangled filaments may provide an easier access to nutrients in such an environment. Based on [Sim et al., 2012], the correlation of an increase in the non-cyanobacterial population with the decrease in upward motility and enhanced cyanobacterial clumping indicates a change in metabolic cycling within the community.

4.2 Future Work

Future results may provide further insight into the mechanisms responsible for and the role of heterotrophic bacteria in conical structures. Further investigation of the correlation between cone formation and the relative heterotrophic population concentration in filamentous cyanobacterial communities needs to be conducted via enrichment and heterotrophic bacteria mixtures as in Section 3.2. Future work should include enrichment mixtures conducted in triplicate as well as confocal microscopy to elucidate the presence and distribution of cyanobacteria and heterotrophic bacteria within cultures.

Chapter 5

Appendix A: Other Methods for Selection

5.1 Selection and Characterization of Cyanobacteria

Using the technique of enrichment via antibiotic selection was successfully enriched for cyanobacteria (NB2) with novobiocin. Other strains were successfully enriched in the first round of selection with colistin and chloramphenicol; however, the samples did not continue to grow upon exposure to a new antibiotic disc. This may have been partly due to weakened antibiotic disc strength. The 16S rDNA analysis of the antibiotic selection is shown in Table 3.2. The antibiotic-selected sample is enriched in cyanobacteria, but more than one unique strain may be present. Thus, while antibiotic-selection successfully enriched in cyanobacteria, we were unable to isolate a single cyanobacterium strain from the bacterial community. However, our results show that phototactic enrichment favors cyanobacterium, *Leptolyngbya*.

Another method, flow cytometry, was used to attempt to select cells in medium filtered from the NB2 enrichment sample. Cells were dispersed to a culture plate *in vitro* as a single cell in groups of three or ten. At least two culture plates (20 single-cells/groups) were made for each of the dispersal amounts. Single-cell growth after three weeks of incubation

at 45° C was not observed. For cells dispersed in groups, growth is observed but did not have morphological similarity to filamentous cyanobacteria. Microscopic analysis was conducted using cyanobacterial pigment fluorescence observable by the Zeiss Axioplan Microscope. Possible growths were re-inoculated on new culture plates using Luria-Bertani (LB) broth and aerobic medium agar solutions, but no further growth was observed.

5.2 Isolation of Heterotrophic Bacteria

Isolation was attempted on samples metabolizing carbon, glucose, fructose, glycol acid, and LB broth, but isolates were only visually detected with LB broth.

Chapter 6

Appendix B: Growth Conditions & Observations of Cyanobacterial Community Enrichment Cultures

^a We characterize culture enrichments of 1, 8 and 14 under varied conditions of light, water depth, and oxygenation.

6.1 Standard Conditions

Under nominal growth conditions (aerobic, 60 E/m²/s, 100 mL medium) , enrichment 1 produces visible surface growth within the first week and forms gas pockets (sub-centimeter scale) beneath the solid substrate surface (see Fig 6-1) that are present for at least two weeks. Based on [Bosak et al., 2010], we presume these gas pockets are oxygen rich. By the third week, millimeter-scale dark green cones and ridges are visible, although a mat and aggregate growth in the water column are not present.

For enrichment 8, within the first few days mass aggregates (clumps) are present on the surface and within the water column along with a thin mat on the solid substrate surface.

^aPart of this subsection was published in [Bosak et al., 2012].

Bubbles are also observable at the surface. Within the next few weeks, thin filamentous sheets are formed that float within the water column along with string-like structures (see Fig 6-2). Enrichment 8 also exhibits fairly homogeneous surface growth, although no cones are formed.

Similar to enrichment 8, enrichment 14 forms many clumps within the water column and on the surface within the first week although surface growth is limited and heterogeneously distributed. Within the next few weeks, growth in the water column remains stable although the growth becomes homogeneously distributed across the surface in addition to a few cones and tufts forming at the surface (see Fig 6-3).

6.2 Low Light

Under the low light condition ($10 \text{ E/m}^2/\text{s}$), enrichment 1 has extremely limited surface growth within the first week. Within the next few weeks, fairly homogenous growth develops across the surface and filamentous filmy sheets attach to the sides of the culture container; few clumps are present in water column. No cones are present by the fourth week, although large clumps are spread across the surface.

Enrichment 8 develops homogenous surface growth within the first week along with gas-filled bubbles. There are few clumps within the water column, considerably less than were present under nominal growth conditions. Over the following weeks, a well-covered, networked surface growth develops absent of cones. Gas pockets and bubbles are present beneath and at the surface along with string-like structures in the water column similar to the networks present on the surface.

Enrichment 14 has limited surface growth throughout the first three weeks although clumps are present on the side of the culture container. Eventually, enrichment 14 develops homogeneous surface growth with large, isolated clumps at the surface and within the water column. No cones are present.

The light-oriented growth of each enrichment at low water depths indicates that the photo-

taxis is a factor, and has a stronger influence at a low water level. This may be due to the less scattering of light associated with lower water levels.

6.3 Low Water Depth

At a low water depth (25-mL medium), enrichment 1 begins with limited, heterogeneous surface growth. The uni-directional surface growth appears to be a phototactic response, with more growth near the light source and surface structures oriented toward the light source. By the second week, cones form that are oriented toward the light and the density of cones increases nearer to the light source. In the third week, filmy sheets form within the water column and on sides of culture container.

Similar to enrichment 1, enrichment 8 begins with limited, heterogeneous and light-oriented surface growth. By the second week, a few isolated clumps are in the water column and many have formed on the surface. Enrichment 8 develops light-oriented, dark-green cones with a greater density of cones nearer to the light source and by the fourth week many clumps are present on the surface and filmy sheets are attached to the side of the culture container. Cones are homogeneously distributed throughout the culture.

Enrichment 14 also begins with limited heterogeneous, uni-directional, surface growth. By the second week, enrichment 14 forms filmy sheets near the light source with clumps in the water column and gas pockets and bubbles throughout the culture surface. A homogenous, smoothly textured surface mat is formed with gas pockets over the next few weeks and no cones are present by the end of the fourth week.

6.4 Anaerobic

Under anaerobic conditions, enrichment 1 begins by developing homogenous surface growth with isolated clumps throughout. By the second week, dark-green cones are formed that are evenly distributed across the surface. Enrichment 8 develops a homogenous mat within the

first week and over the next few weeks the mat is thickened along with the formation gas pockets and bubbles being present at the surface. Enrichment 14 exhibits heterogeneous, unattached surface growth within the first week. Within the next few weeks, centimeter-scale fluffy and tufted cones develop in isolated groups across the surface without an interstitial mat.

6.5 Microscopy

With microscopy (see Figure 3-4), we observe that enrichment 1 is homogeneously entangled in a thick, dense layer. Enrichment 1 is similar to 12 and 14, with the exception that enrichments 12 and 14 have a heterogeneous thickness and enrichment 14 has few regions where the filaments are aligned. Enrichment 8 noticeably clumps at the microscale; this may be a contributing factor to the ability of enrichment 8 to readily clump at the macroscopic level. Additionally, the cyanobacterium in enrichment 8 has an average length of $5.3\mu\text{m}$, about $2\mu\text{m}$ greater than the cyanobacteria of enrichments 1 and 14 and this may also be a contributing factor in the ability of enrichment 8 to more readily form clumps (Table 6.1).

The cyanobacterium in enrichment 8 has an average length of $5.3\mu\text{m}$, about $2\mu\text{m}$ greater than the cyanobacteria of enrichments 1 and 14 and may be a contributing factor in the ability of enrichment 8 to more readily form clumps (Table 6.1).

Enrichment 1

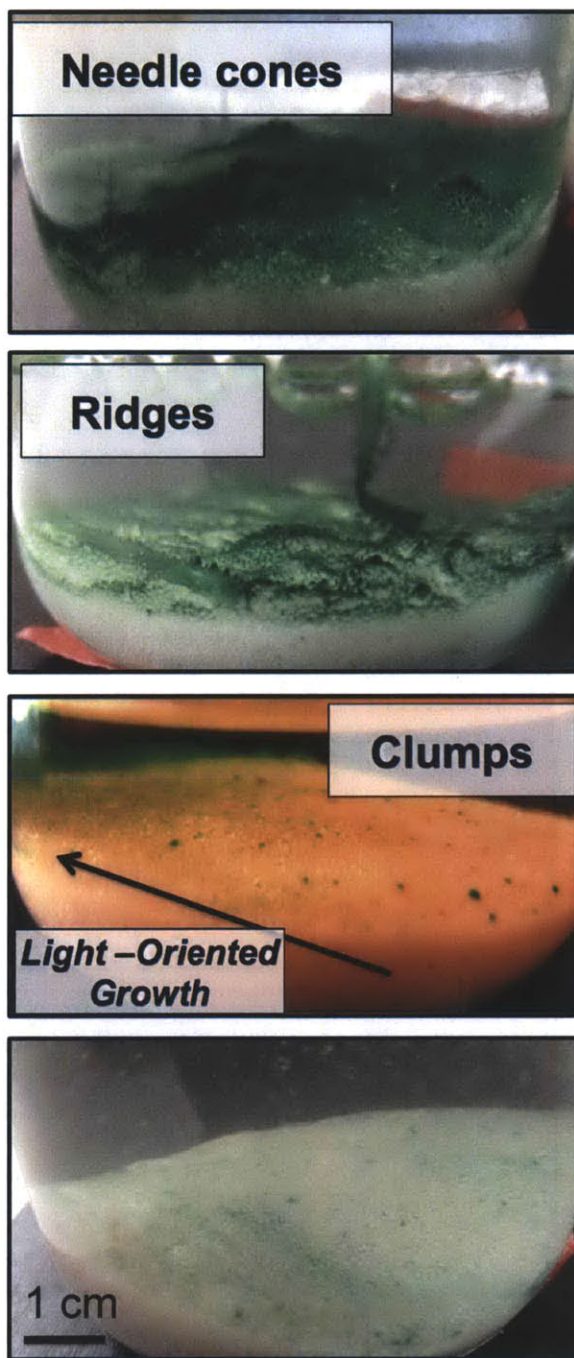


Figure 6-1: Enrichment 1 (14-day incubation). Growth of enrichment 1 at nominal aerobic, low water anaerobic, low water aerobic, and low light aerobic conditions, respectively.

Enrichment 8

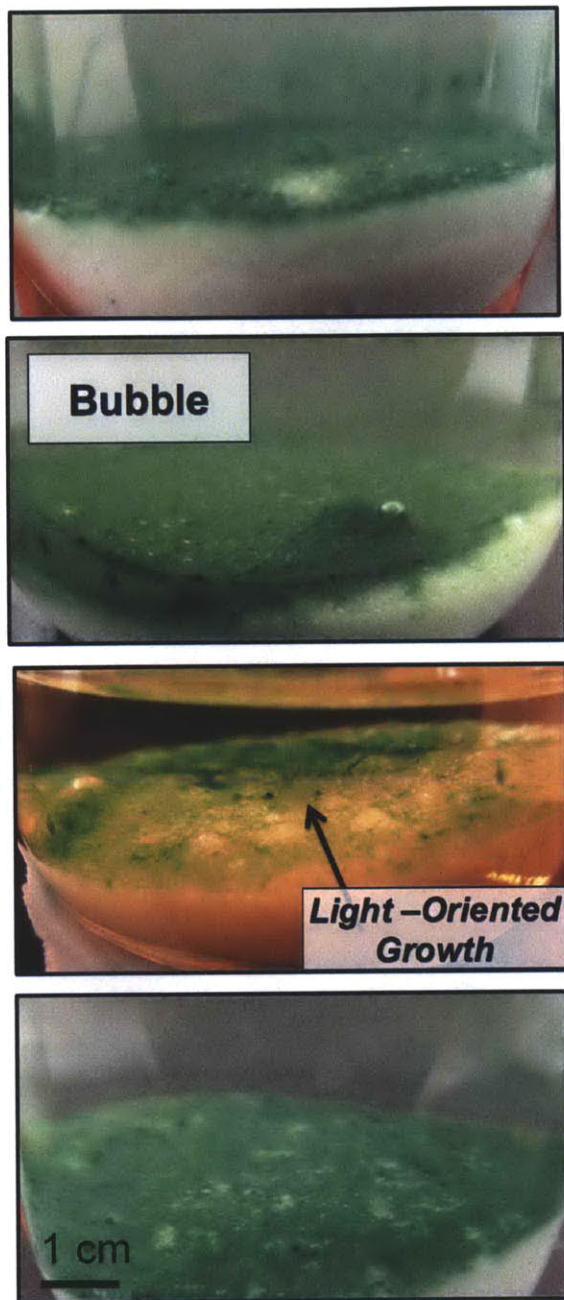


Figure 6-2: Enrichment 8 (14-day incubation). Growth of enrichment 8 is shown at nominal aerobic, low water anaerobic, low water aerobic, and low light aerobic conditions, respectively.

Enrichment 14

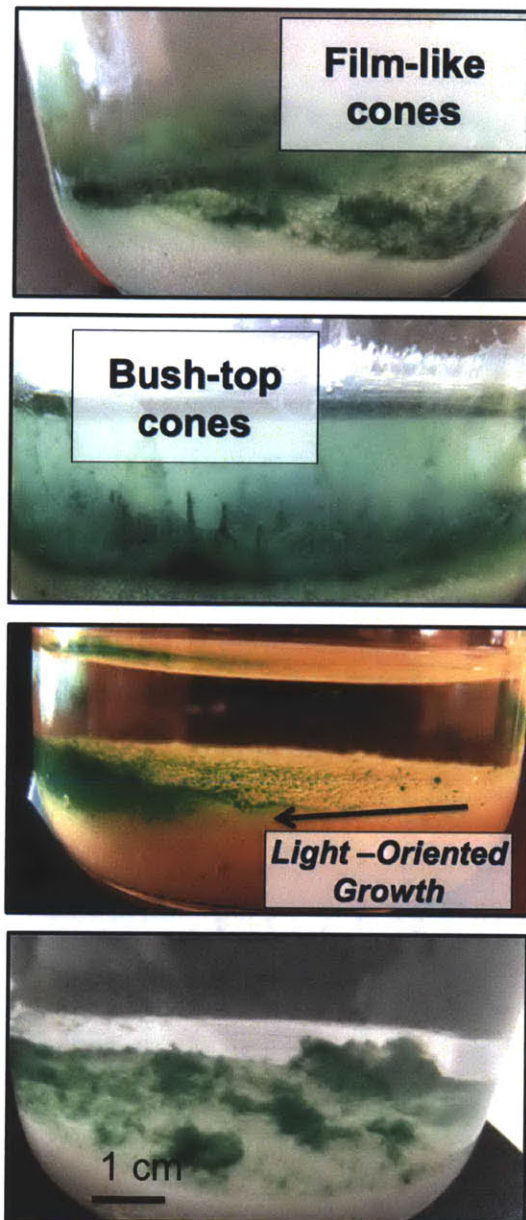


Figure 6-3: Enrichment 14 (14-day incubation). Growth of enrichment 14 is shown at nominal aerobic, low water anaerobic, low water aerobic, and low light aerobic conditions, respectively.

Table 6.1: Average filament length

Sample ID	Average Length μm	Confidence Interval	Count
1	3.42	$\pm 0.08(95\%)$	157
8	5.27	$\pm 0.36(95\%)$	111
14	3.38	$\pm 0.18(95\%)$	126

Bibliography

- [Altermann and Schopf, 1995] Altermann, W. and Schopf, J. W. (1995). Microfossils from the Neoarchean Campbell Group, Griqualand West Sequence of the Transvaal Supergroup, and their paleoenvironmental and evolutionary implications. *Precambrian Research*, 75(1–2):65–90.
- [Awramik and Riding, 1988] Awramik, S. and Riding, R. (1988). Role of algal eukaryotes in subtidal columnar stromatolite formation. *Proceedings of the National Academy of Sciences*, 85(5):1327–1329.
- [Awramik and Vanyo, 1986] Awramik, S. and Vanyo, J. (1986). Heliotropism in modern stromatolites. *Science*, 231(4743):1279–1281.
- [Awramik, 1992] Awramik, S. M. (1992). The oldest records of photosynthesis. *Photosynthesis Research*, 33(2):75–89.
- [Bosak et al., 2010] Bosak, T., Bush, J. W. M., Flynn, M. R., Liang, B., Ono, S., Petroff, A. P., and Sim, M. S. (2010). Formation and stability of oxygen-rich bubbles that shape photosynthetic mats. *Geobiology*, 8(1):45–55.
- [Bosak et al., 2013] Bosak, T., Knoll, A. H., and Petroff, A. P. (2013). The Meaning of Stromatolites. *Annual Review of Earth and Planetary Sciences*, 41(1):21–44.
- [Bosak et al., 2009] Bosak, T., Liang, B., Sim, M. S., and Petroff, A. P. (2009). Morphological record of oxygenic photosynthesis in conical stromatolites. *Proceedings of the National Academy of Sciences*, 106(27):10939–10943.
- [Bosak et al., 2012] Bosak, T., Liang, B., Wu, T. D., Templer, S. P., Evans, A., Vali, H., Guerquin-Kern, J. L., Klepac-Ceraj, V., Sim, M. S., and Mui, J. (2012). Cyanobacterial diversity and activity in modern conical microbialites. *Geobiology*, 10(5):384–401.
- [Burne and Moore, 1987] Burne, R. V. and Moore, L. S. (1987). Microbialites: Organosedimentary Deposits of Benthic Microbial Communities. *Palaios*, 2(3):241.
- [Burton and Lee, 1978] Burton, S. D. and Lee, J. D. (1978). Improved Enrichment and Isolation Procedures for Obtaining Pure Cultures of Beggiatoa. *Applied and Environmental Microbiology*, 35(3):614–617.
- [Castenholz, 1970] Castenholz, R. W. (1970). Laboratory culture of thermophilic cyanophytes. *Schweizerische Zeitschrift für Hydrologie*, 32(2):538–551.

- [Dupraz and Visscher, 2005] Dupraz, C. and Visscher, P. T. (2005). Microbial lithification in marine stromatolites and hypersaline mats. *Trends in Microbiology*, 13(9):429–438.
- [Foster et al., 2009] Foster, J. S., Green, S. J., Ahrendt, S. R., Golubic, S., Reid, R. P., Hetherington, K. L., and Bebout, L. (2009). Molecular and morphological characterization of cyanobacterial diversity in the stromatolites of Highborne Cay, Bahamas. *The ISME Journal*, 3(5):573–587.
- [Gallagher et al., 2004] Gallagher, J. M., Carton, M. W., Eardly, D. F., and Patching, J. W. (2004). Spatio-temporal variability and diversity of water column prokaryotic communities in the eastern North Atlantic. *FEMS Microbiology Ecology*, 47(2):249–262.
- [Gischler et al., 2008] Gischler, E., Gibson, M. A., and Oschmann, W. (2008). Giant Holocene Freshwater Microbialites, Laguna Bacalar, Quintana Roo, Mexico. *Sedimentology*, 55(5):1293–1309.
- [Goh et al., 2008] Goh, F., Allen, M. A., Leuko, S., Kawaguchi, T., Decho, A. W., Burns, B. P., and Neilan, B. A. (2008). Determining the specific microbial populations and their spatial distribution within the stromatolite ecosystem of Shark Bay. *The ISME Journal*, 3(4):383–396.
- [Grotzinger and Knoll, 1999] Grotzinger, J. and Knoll, A. (1999). Stromatolites in Precambrian carbonates: evolutionary mileposts or environmental dipsticks? *Annual Review of Earth and Planetary Sciences*, 27(1):313–358.
- [Hagerthey et al., 2006] Hagerthey, S. E., William Louda, J., and Mongkronsri, P. (2006). Evaluation of Pigment Extraction Methods and a Recommended Protocol for Periphyton Chlorophyll a Determination and Chemotaxonomic Assessment. *J. Phycol*, 42(5):1125–1136.
- [Hoefel et al., 2005] Hoefel, D., Monis, P. T., Grooby, W. L., Andrews, S., and Saint, C. P. (2005). Culture-Independent Techniques for Rapid Detection of Bacteria Associated with Loss of Chloramine Residual in a Drinking Water System. *Applied and Environmental Microbiology*, 71(11):6479–6488.
- [Hofmann et al., 1999] Hofmann, H., Grey, K., Hickman, A., and Thorpe, R. (1999). Origin of 3.45 Ga coniform stromatolites in Warrawoona Group, Western Australia. *Bulletin of the Geological Society of America*, 111(8):1256–1262.
- [Hofmann, 1973] Hofmann, H. J. (1973). Stromatolites: characteristics and utility. *Earth Science Reviews*, 9:339–373.
- [Jones et al., 2002] Jones, B., Renaut, R., Rosen, M., and Ansdell, K. (2002). Coniform Stromatolites from Geothermal Systems, North Island, New Zealand. *Palaios*, 17(1):84–103.
- [Lau et al., 2005] Lau, E., Nash, C., Vogler, D., and Cullings, K. (2005). Molecular diversity of cyanobacteria inhabiting coniform structures and surrounding mat in a Yellowstone hot spring. *Astrobiology*, 5(1):83–92.

- [Petroff et al., 2013] Petroff, A. P., Beukes, N. J., Rothman, D. H., and Bosak, T. (2013). Biofilm growth and fossil form. *Proceedings of the National Academy of Sciences*.
- [Petroff et al., 2010] Petroff, A. P., Sim, M. S., Maslov, A., Krupenin, M., Rothman, D. H., and Bosak, T. (2010). Biophysical basis for the geometry of conical stromatolites. *Proceedings of the National Academy of Sciences*, 107(22):9956–9961.
- [Reyes et al., 2013] Reyes, K., Gonzalez, N. I., Stewart, J., Ospino, F., Nguyen, D., Cho, D. T., Ghahremani, N., Spear, J. R., and Johnson, H. A. (2013). Surface Orientation Affects the Direction of Cone Growth by *Leptolyngbya* sp. Strain C1, a Likely Architect of Coniform Structures Octopus Spring (Yellowstone National Park). *Applied and . . .*
- [Sim et al., 2012] Sim, M. S., Liang, B., Petroff, A. P., Evans, A., Klepac-Ceraj, V., Flannery, D. T., Walter, M. R., and Bosak, T. (2012). Oxygen-Dependent Morphogenesis of Modern Clumped Photosynthetic Mats and Implications for the Archean Stromatolite Record. *Geosciences*, 2(4):235–259.
- [Vaara et al., 1979] Vaara, T., Vaara, M., and Niemela, S. (1979). Two improved methods for obtaining axenic cultures of cyanobacteria. *Applied and Environmental Microbiology*.
- [Walter et al., 1976a] Walter, M. R., Bauld, J., and Brock, T. D. (1976a). Chapter 6.2 Microbiology and Morphogenesis of Columnar Stromatolites (Conophyton, Vacerrilla) from Hot Springs in Yellowstone National Park. In Walter, M. R., editor, *Stromatolites*, pages 273–310. Elsevier.
- [Walter et al., 1976b] Walter, M. R., GOODE, A. D. T., and HALL, W. D. M. (1976b). Microfossils from a newly discovered Precambrian stromatolitic iron formation in Western Australia. *Nature*, 261(5557):221–223.
- [Ward et al., 1997] Ward, D., Santegoeds, C., Nold, S., Ramsing, N., Ferris, M., and Bateson, M. (1997). Biodiversity within hot spring microbial mat communities: molecular monitoring of enrichment cultures. *Antonie van Leeuwenhoek*, 71(1):143–150.
- [Wharton et al., 2013] Wharton, Jr, R. A., Parker, B. C., and Simmons, G. M. (2013). Distribution, species composition and morphology of algal mats in Antarctic dry valley lakes. *Phycologia*, 22(4):355–365.